Design, Synthesis, and Biological Evaluation of 1,4-Diaryl-1,4-dihydropyrazines as Novel 11β-HSD1 Inhibitors

Xiaowei Duan, Hongxing Xin, and Hong Yan*

College of Life Science and Bio-engineering, Beijing University of Technology; Pingleyuan Street No. 100, Chaoyang District, Beijing 100124, P.R. China.

Received January 22, 2014; accepted February 20, 2014

The inhibition of 11β-hydroxysteroid dehydrogenase type 1 (11β-HSD1) has demonstrated potential for the treatment of various components of metabolic syndrome. In this study, a series of 1,4-diaryl-1,4-dihydropyrazines were designed as inhibitors of 11β-HSD1 based on the structure–activity relationship of known 11β-HSD1 inhibitors through docking simulations. The docking simulation results supported the initial pharmacophore hypothesis: the docking results of the known inhibitors with 11β-HSD1 suggested a similar interaction of 1,4-diaryl-1,4-dihydropyrazines with the catalytic site of 11β-HSD1. Twelve of these compounds were synthesized through the cyclization of *N*,*N*-dialkylanilines with anilines, and their structures were determined by ^{1}H-NMR, ^{13}C-NMR, high resolution (HR)-MS, and single-crystal X-ray diffraction. The inhibitory activities of these compounds against human 11β-HSD1 were investigated *in vitro* through a scintillation proximity assay using microsomes containing 11β-HSD1.

Key words 1,4-diaryl-1,4-dihydropyrazine; synthesis; structure–activity relationship; 11β-hydroxysteroid dehydrogenase type 1 (11β-HSD1) inhibitor

11β-Hydroxysteroid dehydrogenase type 1 (11β-HSD1) is a reduced nicotinamide adenine dinucleotide phosphate (NADPH)-dependent reductase responsible for catalyzing the conversion of inactive cortisone into active glucocorticoid cortisol.[1] Excessive levels of glucocorticoids can cause metabolic syndrome, including insulin resistance, visceral obesity, and type 2 diabetes.[2–5] Thus, 11β-HSD1 is hypothesized to be critical for the development of metabolic syndrome.[6] In the past few years, researchers have designed and synthesized a large number of 11β-HSD1 inhibitors, such as arylsulfonyl piperazine **1**, benzenesulfonamide **2**, and diaryl sulfone **3**[7–10] (Fig. 1).

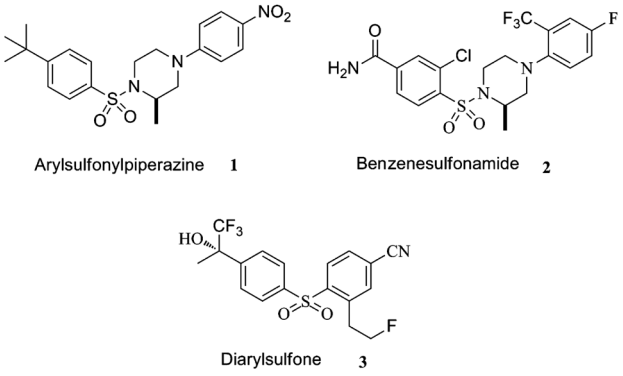

Fig. 1. Representative 11β-HSD1 Inhibitors

Based on the molecular modeling of the interactions between the known inhibitors and 11β-HSD1, the development of small-molecule inhibitors of 11β-HSD1 was initiated with 1,4-dihydropyrazines. The interaction of the designed 1,4-diaryl-1,4-dihydropyrazines (**4**) with the catalytic site of 11β-HSD1 was similar to that of the known inhibitors (Fig. 2). The molecular structure of **4** can fold at an angle of 107.18–113.15° into a V shape and has the potential to fit into the enzyme's V-shaped hydrophobic pocket. To test this hypothesis, a series of **4** was synthesized through the cyclization of *N*,*N*-dialkyl aniline with aniline in the presence of catalytic hydrochloride (Chart 1). The inhibition of 11β-HSD1 by the enzymatic activities of **4** was determined through a scintillation proximity assay using microsomes containing 11β-HSD1.[11,12]

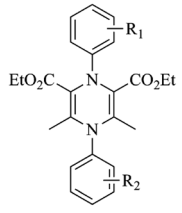

Fig. 2. Structure of 1,4-Diaryl-1,4-dihydropyrazine **4**

RESULTS AND DISCUSSION

Structure Designs Based on the X-ray crystal structure of 11β-HSD1-inhibitor complexes (PDB code: 3H6K),[13] AutoDock 4.0 (Scripps Research Institute, La Jolla, CA, U.S.A.) was used to simulate the known inhibitors (**1**–**3**) and **4** with 11β-HSD1. As illustrated in Fig. 3, the known inhibitors, which contain two hydrophobic groups at the two terminals and double-bonded oxygen in the middle of the structure, adopted a V-shaped crystal structure in the docking models. A detailed examination of the inhibitor binding site of 11β-HSD1 with **1**, **2**, and **3** showed that the hydrogen bond donated by sulfonyl oxygen with Tyr183 and the enzyme's V-shaped hydrophobic pockets, which contain residues 170 to 220, are critical for the inhibitory effect in the catalytic cycle. For example, the docking models of **1**, **2**, and **3** with 11β-HSD1 reveal that the amido hydrogen of Tyr183 donates a hydrogen bond to the sulfonyl oxygen and the molecules are folded at an angle of 100.71°, 100.11° and 106.11° into a V shaped to match

The authors declare no conflict of interest.

* To whom correspondence should be addressed. e-mail: hongyan@bjut.edu.cn

© 2014 The Pharmaceutical Society of Japan

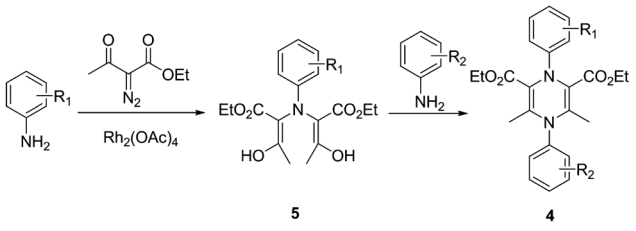

4-1: R_1=H, R_2=H; **4-2**: R_1=H, R_2=4-Cl; **4-4**: R_1=H, R_2=4-CH_3; **4-10**: R_1=4-Cl, R_2=H; **4-11**: R_1=4-Cl, R_2=4-Cl; **4-12**: R_1=4-Cl, R_2=4-CH_3; **4-14**: R_1=4-Cl, R_2=4-OCH_3; **4-19**: R_1=CH_3, R_2=H; **4-20**: R_1=4-CH_3, R_2=4-C; **4-24**: R_1=4-CH_3, R_2=4-OCH_3; **4-60**: R_1=$COOC_2H_5$, R_2=4-$COOC_2H_5$; **4-61**: R_1=3-NO_2, R_2=3-NO_2

Chart 1. Synthesis of 1,4-Diaryl-1,4-dihydropyrazines **4**

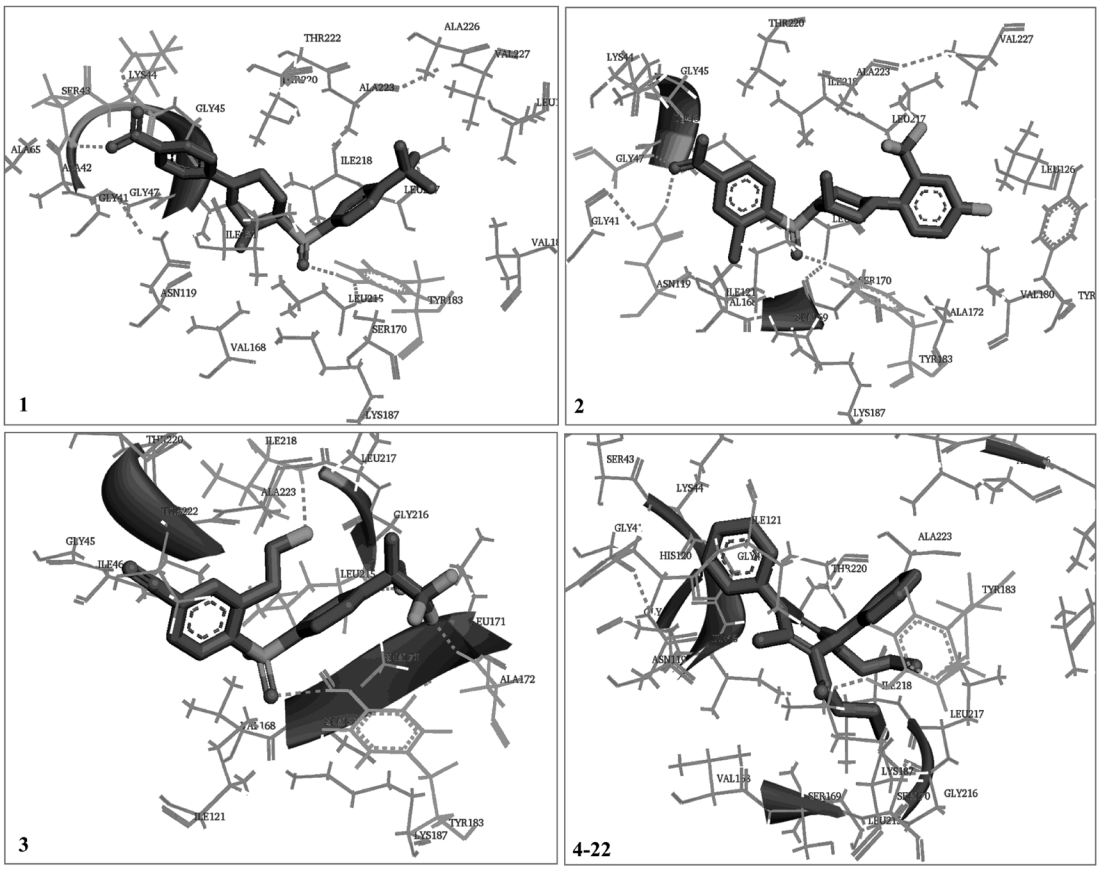

Fig. 3. The Binding Mode of **1**, **2**, **3**, and **4-22** to Human 11β-HSD1 (PDB Code: 3H6K)

The amino acid residues forming hydrogen bonds with molecules are shown in green, the hydrogen bond in red dashed.

the cavity of the enzyme's active site. In these cases, sulfonyls are presumed to donate hydrogen bonds to the catalytic site. To better fit into the enzymatic active site, these compounds adjust their configurations to a V shape with an angle that ranges from 100° to 115°.

The docking of 1,4-diphenyl-dihydropyrazine **4-22** with 11β-HSD1 using the same method used for the docking of **1**, **2** and **3** revealed that the carbonyl oxygen of the ester of **4-22** accepts a hydrogen bond from the amides of Tyr183, as was observed with the known inhibitors. The hydrophobic aryl at the N1 and N4 positions of the pyrazine ring can be modulated to fit the V-shaped hydrophobic pocket of the enzyme. The stacked plots between 1,4-diphenyl-1,4-dihydropyrazines and the known inhibitors are very similar.

More than 60 of the 1,4-diaryl-1,4-dihydropyrazines (**4**) were grown *in silico* through the addition of different substituent groups to the phenyl substituent and docked with 11β-HSD1. The docking results are shown in Table 1.

As shown in Table 1, compounds **4** exhibit a better binding capacity with 11β-HSD1 compared with the known inhibitors; in fact, the free energy values ΔG and inhibition constant values K_i of most compounds **4** are between −8.48 and −5.49 kcal/mol and between 0.605 and 131.72 μM, respectively. The binding capacities of the V-shaped **4** were similar to those obtained from the re-docking of **1**, **2**, and **3** (ΔG=−9.25, −6.73, and −6.10 kcal/mol, K_i=0.166, 11.63, and 33.88 μM, respectively). The hydrophilic and the steric effect of the substituents (R_1 and R_2) were speculated to affect the binding capacity. The docking results obtained with hydrophilic substituents are better than those obtained with hydrophobic substituents, such as **4-64** (R_1=4-COOH, R_2=4-OH, ΔG=−7.81 kcal/mol, K_i=1.88 μM) and **4-31** (R_1=4-CF_3, R_2=4-CF_3, ΔG=−5.29 kcal/

Table 1. Molecular Docking Results of **4** and the Known Inhibitors with 11β-HSD1

Compound	R_1	R_2	$\Delta G^{a)}$ (kcal/mol)	$K_i^{b)}$ (μM)
4-1	H	H	−6.95	8.02
4-2	H	4-Cl	−7.16	5.68
4-3	H	4-OH	−6.94	8.14
4-4	H	4-CH_3	−7.07	6.56
4-5	H	4-CF_3	−6.19	28.98
4-6	H	4-OCH_3	−6.56	15.64
4-7	H	4-CH_2OH	−6.44	19.04
4-8	H	4-COOH	−7.54	2.95
4-9	H	4-$COOC_2H_5$	−5.73	63.24
4-10	4-Cl	H	−6.44	19.04
4-11	4-Cl	4-Cl	−6.89	8.90
4-12	4-Cl	4-CH_3	−6.81	10.18
4-13	4-Cl	4-CF_3	−6.23	27.10
4-14	4-Cl	4-OCH_3	−6.81	10.17
4-15	4-Cl	4-CH_2OH	−6.64	13.59
4-16	4-Cl	4-COOH	−7.77	2.02
4-17	4-Cl	4-$COOC_2H_5$	−6.25	26.26
4-18	4-OH	4-OH	−7.15	5.79
4-19	4-CH_3	H	−7.00	7.38
4-20	4-CH_3	4-Cl	−7.57	2.83
4-21	4-CH_3	4-OH	−7.26	4.79
4-22	4-CH_3	4-CH_3	−7.08	6.43
4-23	4-CH_3	4-CF_3	−6.34	22.71
4-24	4-CH_3	4-OCH_3	−6.51	16.96
4-25	4-CH_3	4-CH_2OH	−6.75	11.22
4-26	4-CH_3	4-$COOC_2H_5$	−6.16	30.62
4-27	4-CF_3	H	−5.82	53.73
4-28	4-CF_3	4-Cl	−5.84	52.62
4-29	4-CF_3	4-OH	−5.63	74.23
4-30	4-CF_3	4-CH_3	−5.68	68.86
4-31	4-CF_3	4-CF_3	−5.29	131.73
4-32	4-CF_3	4-OCH_3	−5.49	94.02
4-33	4-CF_3	4-CH_2OH	−5.19	157.74
4-34	4-CF_3	4-COOH	−6.79	10.61
4-35	4-CF_3	4-$COOC_2H_5$	−5.64	73.78
4-36	4-CH_2OH	H	−7.78	2.00
4-37	4-CH_2OH	4-Cl	−7.32	4.27
4-38	4-CH_2OH	4-OH	−7.03	7.01
4-39	4-CH_2OH	4-CF_3	−6.04	37.58
4-40	4-CH_2OH	4-OCH_3	−7.11	6.19
4-41	4-CH_2OH	4-CH_2OH	−6.56	15.60
4-42	4-CH_2OH	4-COOH	−7.45	3.46
4-43	4-CH_2OH	4-$COOC_2H_5$	−5.94	44.10
4-44	4-COOH	H	−8.01	1.35
4-45	4-COOH	4-Cl	−8.03	1.30
4-46	4-COOH	4-OH	−7.81	1.88
4-47	4-COOH	4-CH_3	−8.48	0.605
4-48	4-COOH	4-CF_3	−5.65	72.02
4-49	4-COOH	4-OCH_3	−6.55	15.70
4-50	4-COOH	4-CH_2OH	−8.08	1.19
4-51	4-COOH	4-COOH	−7.81	1.88
4-52	4-COOH	4-$COOC_2H_5$	−6.24	26.83
4-53	4-$COOC_2H_5$	H	−6.38	21.14
4-54	4-$COOC_2H_5$	4-Cl	−6.00	39.87
4-55	4-$COOC_2H_5$	4-OH	−5.68	68.60
4-56	4-$COOC_2H_5$	4-CH_3	−6.19	29.02
4-57	4-$COOC_2H_5$	4-CF_3	−6.09	34.57
4-58	4-$COOC_2H_5$	4-OCH_3	−5.80	56.48
4-59	4-$COOC_2H_5$	4-CH_2OH	−5.92	45.48
4-60	4-$COOC_2H_5$	4-$COOC_2H_5$	−6.11	12.56
4-61	3-NO_2	3-NO_2	−6.74	11.58
1	—	—	−9.25	0.166 (0.003$^{c)}$)
2	—	—	−6.73	11.63 (0.063$^{c)}$)
3	—	—	−6.10	33.88 (0.012$^{c)}$)

a) Binding free energy. *b*) Inhibition constant. *c*) Experimental value (μM).

mol, K_i=131.73 μM). If the R is a small group, such as H, 4-Cl, and 4-CH_3, the values of K_i are between 0.65 and 19.04 μM and similar to those of the known inhibitors, as was observed with **4-20** (R_1=4-CH_3, R_2=4-Cl, ΔG=−7.57 kcal/mol, K_i=2.83 μM). If *R* is a large group, such as 4-$CO_2CH_2CH_3$, the values of K_i are between 12.56 and 68.60 μM and slightly larger than those of the known inhibitors, as was observed with **4-58** (R_1=4-$COOC_2H_5$, R_2=4-OCH_3, ΔG=−5.80 kcal/mol, K_i=56.48 μM), which might explain why the ethoxycarbonyl group is too large to fit the V-shaped cavity of 11β-HSD1.

Synthesis of 1,4-Diaryl-1,4-dihydropyrazine Based on previously reported reaction conditions,[14] the 1,4-diaryl-1,4-dihydropyrazines **4** were synthesized through the cyclization reactions of *N*,*N*-dialkyl-anilines **5** with anilines, as depicted in Chart 1. The intermediates **5** were prepared by the *N*-alkylation of aniline with ethyl 2-diazo acetoacetate in the presence of catalytic rhodium acetate dimer. Under a nitrogen atmosphere, intermediates **5** were obtained at acceptable yields (49–69%). It is worth mentioning that an amount of by-product is generated by the oxidation of some intermediates that are not isolated from air.[15] The synthesis of 4-aryl-1,4-dihydropyrazine reported by Chorvat and Rorig[14] and improved by Sit *et al.*[16] and He *et al.*[15] was used for the cyclization of *N*,*N*-bisalkylated anilines **5** with ammonium acetate. To determine the synthesis mechanism of 1,4-diaryl-1,4-dihydropyrazines **4**, **4-1** was used as a reactant in a model reaction (Chart 1). The cyclization of *N*,*N*-bisalkylated anilines **5** with anilines yielded **4-1** at markedly lower yields. The use of a proton or Lewis acid as the catalyst produced **4-1** at higher yields (Table 2). The catalyst amount was 0.2–0.4 mol% based on the synthesis of 1,4-dihydropyridines.[17]

The data in Table 2 show that the use hydrochloric acid (HCl) as the catalyst synthesizes **4-1** in the least time (3.5 h) and at the highest yield (58%) compared with the other acid catalysts tested. The catalytic mechanism through which **4-1** formed is thus likely similar to that responsible for the synthesis of 1-aryl-1,4-dihydropyridines.[16,17] In the presence of hydrochloric acid as the catalyst, the hydroxyl of **5** was easily protonated and thus easily cyclized with aniline. Based on the synthesis mechanism of **4-1**, a series of compounds **4** was synthesized by the cyclization of bis-alkylated anilines in the presence of catalytic hydrochloride (Table 3).

The structures of **4** were confirmed by ^{1}H-NMR, ^{13}C-NMR, high resolution (HR)-MS, and single-crystal X-ray diffraction. Compound **4-1** will be used as a representative example to discuss the structural details of these compounds. The ^{1}H-NMR spectrum of **4-1** exhibit the signals from the two ethyl methanoate groups as a triplet at δ 1.26 ppm and a quartet at δ 4.26 ppm and the signals from the two methyl groups at δ 2.17 ppm. The signals corresponding to the five protons

Table 2. Yields of **4-1** Catalyzed by Different Acids[a)]

Catalysts	Reaction time (h)	Yield (%)[b)]
Acetic acid	5.0	40
Sulfuric acid	4.5	45
Hydrochloric acid	3.5	58
Zinc chloride	4.0	49

a) Anilines (1.2 mmol), *N*,*N*-dialkylanilines **5b** (1 mmol), catalyst (0.01 mmol), *tert*-butyl alcohol (15 mL) at reflux. *b*) Isolated yields, purified by chromatography on silica gel (petroleum ether–ethyl acetate, 20 : 1).

Table 3. Yields of 1,4-Diaryl-1,4-dihydropyrazines **4**[a)]

Entry	R_1	R_2	Time (h)	Yield[b)] (%)
4-1	H	H	2	56
4-2	H	4-Cl	2	55
4-4	H	4-CH_3	2.5	55
4-10	4-Cl	H	2	63
4-11	4-Cl	4-Cl	1.5	62
4-12	4-Cl	4-CH_3	2.5	60
4-14	4-Cl	4-OCH_3	2.5	59
4-19	4-CH_3	H	3.0	33
4-20	4-CH_3	4-Cl	2	31
4-24	4-CH_3	4-OCH_3	3.5	29
4-60	4-$COOC_2H_5$	4-$COOC_2H_5$	1.5	68
4-61	3-NO_2	3-NO_2	1.5	62

a) Anilines (1.2 mmol), *N*,*N*-dialkylanilines **5** (1 mmol), hydrochloric acid (0.01 mmol), *tert*-butyl alcohol (15 mL) at reflux. *b*) Isolated yields, purified by chromatography on silica gel (petroleum ether–ethyl acetate, 20 : 1).

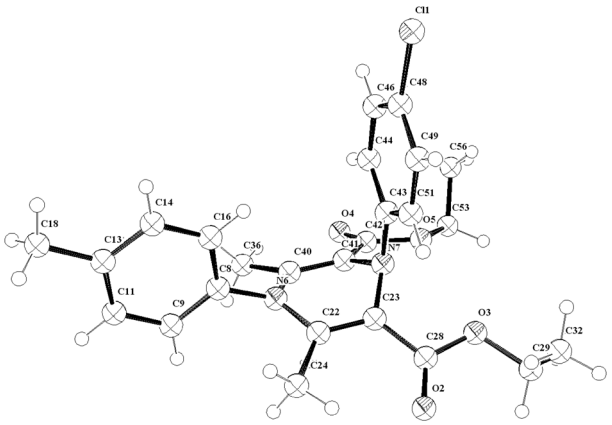

Fig. 4. ORTEP of Compound **4-12** (One of Two Independent Molecules with 50% Probability)

from the benzene group at N1 of **4-1** are in the range of δ 7.17–7.37, and the signals corresponding to the five protons from the benzene group at N4 of **4-1** are in the range of δ 678–6.90. In the ^{13}C-NMR spectra of **4-1**, there are only 14 signals due to the symmetry of the benzene ring and the pyrazine ring. The two carbonyl carbons resides at δ 166.8 ppm, the two signals from the pyrazine ring appear at δ 112.1 and 113.3 ppm, and the eight signals from the two benzene rings are found in the range of δ 128.5–150.5. The remaining signals are ascribed to the two ethoxyl groups and two methyl groups (δ 14.4, 16.4, 60.4 ppm). The HR-MS (electrospray ionization (ESI)) of **4-1** shows a molecular ion peak at 407.1983 *m*/*z*, which is consistent with the calculated 407.1971 *m*/*z* for **4-1** $[M+H]^+$. The single-crystal X-ray diffraction of **4-12** further proves that **4-1** is 3,5-dimethyl-1,4-diphenyl-1,4-dihydropyrazine-2,6-diethylmethanoate (Fig. 4). Structure parameters for **4-12** are given in Table 4 and crystallographic data were deposited with the Cambridge Crystallographic Data Centre under deposition number CCDC 775906.

Biological Activity of 1,4-Diaryl-1,4-dihydropyrazines The inhibitory properties of the synthesized molecules were evaluated through a scintillation proximity assay with human 11β-HSD1 (from HEK293 cells transfected with a full-length pcDNA3-derived expression plasmid). The percentage inhibition of 11β-HSD1 was measured at concentration of 1 μM and

Table 4. Crystal Data and Structure Refinement for **4-12**

Empirical formula	$C_{25}H_{27}ClN_2O_4$
Formula weight	454.94
Temperature	113(2) K
Wavelength	0.71073 Å
Crystal system, space group	Monoclinic, *P*2(1)/*n*
Unit cell dimensions	a=10.160(2)
	b=17.522(4)
	c=13.821(3)
	α=90.00°
	β=104.93(3)°
	γ=90.00°
Volume	1438.3(3) Å^3
Z	4
Calculated density	1.271 g m^{-3}
Absorption coefficient	0.194 mm^{-1}
F(000)	960
θ Range for data collection	1.917–27.906°
Index ranges	$-12\leq h\leq 12$, $-14\leq k\leq 20$, $-16\leq l\leq 16$
Observed reflections	17128
Independent reflections	4184
Data/restraints/parameters	4184/124/328
Goodness-of-fit on F^2	1.1
R indices (all data)	R^1=0.0510, wR^2=0.1416
Extinction coefficient	0.275

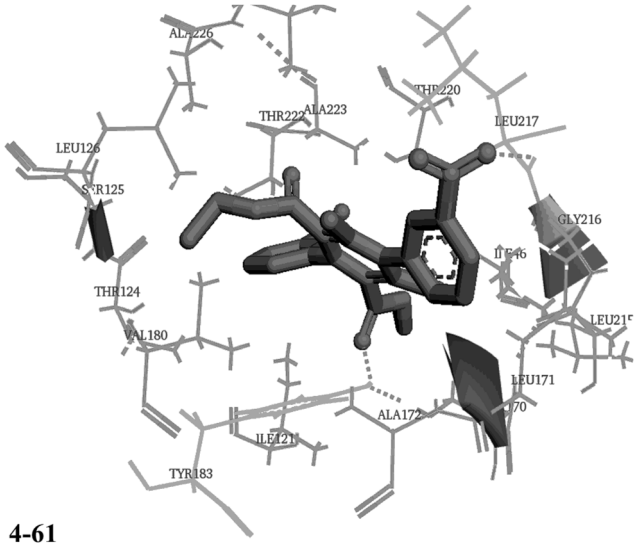

4-61

Fig. 5. The Binding Mode of **4-61** to Human 11β-HSD1 (PDB Code: 3H6K)

The amino acid residues forming hydrogen bonds with molecules are shown in green, the hydrogen bond in red dashed.

10 μM of each molecule. The results showed that **4** exhibited no inhibitory activity at a concentration of 1 μM and inhibited approximately 10% of the 11β-HSD1 enzymatic activity at a concentration of 10 μM. Specifically, **4-11** and **4-61** inhibited more than 20% of the activity of human 11β-HSD1. This result was different from that obtained through molecular docking simulations. Although the V-shaped structure of **4** is similar to that of **1**, **2**, and **3**, the substituents on the aryl group also affect the inhibitory effect of the compound on the activity of 11β-HSD1. The known inhibitors **1**, **2**, and **3** have donating hydrogen-bond groups (–NO_2, –F, and –CN,

respectively) at two terminals, so do **4-11** (4-Cl, 4-Cl) and **4-61** (3-NO_2, 3-NO_2). The docking mode of **4-61** explains the reason of its better inhibitory activities than the other synthesized compounds for its additional hydrogen bonds formed by NO_2 with Leu217 excepts the ester group with Tyr183 (Fig. 5). The biological activities obtained show that the structures of **4** needs to be further modified by changing the hydrophobic properties of R_1 and R_2 into hydrophilic groups to enhance the interaction of the resulting compound with 11β-HSD1.

CONCLUSION

Novel 1,4-diaryl-1,4-dihydropyrazines (**4**) were rationally designed as 11β-HSD1 inhibitors based on docking simulations. The docking results indicated that the novel compounds exhibit a similar V shape and similar ΔG and K_i values to those of the known inhibitors **1**, **2**, and **3**. The compounds **4** were synthesized through the cyclization of *N*,*N*-dialkyl-anilines with anilines in the presence of catalytic hydrochloride at yields in the range of 29 to 68%. The inhibitory activities of these compounds against 11β-HSD1 (microsome fractions from HEK-293 cells) were evaluated. The results showed that most of the compounds inhibited less than 10% of the 11β-HSD1 activity at a concentration of 10 μM, whereas **4-11** (4-Cl, 4-Cl) and **4-61** (3-NO_2, 3-NO_2) inhibited more than 20% of the activity.

MATERIALS AND METHODS

All of the chemicals were used as purchased without further purification. All of the solvents were reagent grade and, when necessary, were purified and dried using standard methods. The melting points were determined using an X-5 apparatus (open capillaries, uncorrected values). The ^{1}H- and ^{13}C-NMR spectra were obtained using a Bruker ARX-400 MHz spectrophotometer, and the chemical shift values are expressed in δ values (ppm) relative to tetramethylsilane (TMS) as the internal standard. The coupling constants are given in Hz, and the signals are quoted as follows: s (singlet), d (doublet), t (triplet), and m (multiplet). All of the compounds were routinely checked by TLC, ^{1}H- and ^{13}C-NMR. TLC was performed using coated silica gel plates (GF254, Haiyang Chemical Plant, Qingdao, China). The developed chromatograms were visualized under ultraviolet light at 254 nm or by iodine vapor.

Molecular Modeling Study The automated docking studies were performed with AutoDock 4.0. This automated ligand-docking program uses the Lamarckian genetic algorithm (LGA) to explore the full range of ligand conformational flexibility with partial flexibility of the receptor. The Lamarckian genetic algorithm is a hybrid of a genetic algorithm and a local search algorithm. This algorithm first builds a population of individuals (genes), in which each gene is a different random conformation of the docked compound. The local search algorithm then performs energy minimizations on a user-specified proportion of the population of individuals. If the energy of the new individual is lower than that of the old individual, the new one is automatically accepted as the next step in the docking simulation.

Preparation of the Receptor and Ligand Molecules The three-dimensional structures of the ligands were constructed using standard bond lengths and bond angles in the GAUSSVIEW 3.09 software (Gaussian, Inc., Wallingford, CT, U.S.A.). The geometry optimizations were conducted using the semi-empirical Austin Model 1 (AM1) method, and the output files were then minimized using the density functional (DFT) method by applying the B3 LYP (Becke, Lee, Yang, and Parr) correlation function during the second optimization. The Gasteiger partial charges were assigned using AutoDock Tools. The crystal structure of human 11β-HSD1 complexed with a sulfonyl-piperazine inhibitor (PDB code: 3H6K) was retrieved from the Brookhaven Protein Data Bank. After the removal of the inhibitor from the complex, the polar hydrogen atoms and the Gasteiger charges were added to the macromolecule.

Modeling and Analysis of the Docked Data For the docking, the size of the receptor grid box was set to 50×50×50, and its grid spacing was 0.375 Å. Given the known location of the sulfonyl-piperazine binding site, the cubic grid box was centered in the catalytically active region, which encompassed the binding site, and the grid center was designated at dimensions *x*, *y*, and *z* of 5.317, 38.734, and −6.249, respectively. The docked conformations were generated using the LGA with an initial population size of 150 structures. The rest of the parameters were set to their default values. The docking assessment depends on the size of the data, the estimated free energy of binding (ΔG bind), and the estimated inhibition constant (K_i). The model analyses were performed using the ACCELRYS DS VISUALIZER 3.0 software (Accelrys, Inc., San Diego, CA, U.S.A.).

General Procedure for the Preparation of *N*,*N*-Dialkylanilines (5) The compound **5** were synthesized by Sing-Yuen Sit method.[16] The aromatic amines (5 mmol) and the rhodium(II) acetate dimer (5.5 mg) were heated at reflux temperature in anhydrous benzene (10 mL) with fast stirring under an atmosphere of nitrogen. A solution of ethyl diazoacetoacetate in anhydrous benzene was then added dropwise. The reaction was monitored by TLC and chromatographed on silica gel (petroleum ether–ethyl acetate, 20 : 1) to provide the *N*,*N*-dialkyl aromatic amines **5**.

Diethyl 2,2′-(Phenylazanediyl)bis(3-hydroxybut-2-enoate) (**5a**): Orange crystals (64%); mp 147.2–148.6°C; ^{1}H-NMR (400 MHz, $CDCl_3$) δ: 1.25 (t, J=7.2 Hz, 6H, $-CO_2CH_2C\underline{H}_3$), 1.68 (s, 6H, CH_3), 4.27 (q, J=7.2 Hz, 4H, $-CO_2C\underline{H}_2CH_3$), 6.94–7.59 (m, 4H, Ar-H), 12.87 (s, 2H, –OH), and 12.90 (s, 1H, –OH).

Diethyl 2,2′-(Phenylazanediyl)bis(3-hydroxybut-2-enoate) (**5b**): Colorless crystals (49%); mp 82.0–82.8°C; ^{1}H-NMR (400 MHz, $CDCl_3$) δ: 1.25 (t, J=7.2 Hz, 6H, $-CO_2CH_2C\underline{H}_3$), 1.85 (s, 6H, CH_3), 4.24 (q, J=7.2 Hz, 4H, $-CO_2C\underline{H}_2CH_3$), 6.63–7.20 (m, 5H, Ar-H), 12.82 (s, 2H, –OH).

Diethyl 2,2′-((4-Chlorophenyl)azanediyl)bis(3-hydroxybut-2-enoate) (**5c**): Colorless crystals (67%); mp 128.1–129.0°C; ^{1}H-NMR(400 MHz, $CDCl_3$) δ: 1.23 (t, J=7.2 Hz, 6H, $-CO_2CH_2C\underline{H}_3$), 1.83 (s, 6H, CH_3), 4.22 (q, J=7.2 Hz, 4H, $-CO_2C\underline{H}_2CH_3$), 6.55–7.12 (m, 4H, Ar-H), 12.79 (s, 2H, –OH).

Diethyl 2,2′-(*p*-Tolylazanediyl)bis(3-hydroxybut-2-enoate) (**5d**): Colorless crystals (45%); mp 46.5–47.7°C; ^{1}H-NMR (400 MHz, $CDCl_3$) δ: 1.25 (t, J=7.2 Hz, 6H, $-CO_2CH_2C\underline{H}_3$), 1.85 (s, 6H, CH_3), 3.80 (s, 3H, Ar-$C\underline{H}_3$), 4.21 (q, J=7.2 Hz, 4H, $-CO_2C\underline{H}_2CH_3$), 6.61–7.12 (m, 4H, Ar-H), 12.80 (s, 2H, –OH).

Diethyl 2,2′-((4-(Ethoxycarbonyl)phenyl)azanediyl)bis(3-hydroxybut-2-enoate) (**5e**): Colorless crystals (69%); mp

105.3–107.9°C; ^{1}H-NMR (400 MHz, $CDCl_3$) δ: 1.23 (t, J=7.2 Hz, 6H, $-CO_2CH_2C\underline{H}_3$), 1.22 (t, J=7.2 Hz, 3H, $-ArCO_2CH_2C\underline{H}_3$), 1.76 (s, 6H, CH_3), 4.20 (q, J=7.2 Hz, 2H, $-ArCO_2C\underline{H}_2CH_3$), 4.14 (q, J=7.2 Hz, 4H, $-CO_2C\underline{H}_2CH_3$), 7.79–7.97 (m, 4H, Ar-H), 12.78 (s, 2H, –OH).

General Procedure for the Preparation of 1,4-Diaryl-1,4-dihydropyrazines (4) The aromatic amines **5** (1.2 mmol) and *N*,*N*-dialkyl aromatic amine (1 mmol) were heated at reflux temperature in *tert*-butyl alcohol (TBA; 15 mL) with fast stirring. Then, 1 mL of hydrochloric acid (0.01 mol/L) was added. The reaction was monitored by TLC and chromatographed on silica gel (petroleum ether–ethyl acetate, 20 : 1) to produce the desired compounds.

3,5-Dimethyl-1,4-diphenyl-1,4-dihydropyrazine-2,6-diethylmethanoate (**4-1**): Light yellow solid (56%); mp 226.5–227.7°C; ^{1}H-NMR (400 MHz, $CDCl_3$) δ: 1.26 (t, J=7.2 Hz, 6H, $-CO_2CH_2C\underline{H}_3$), 2.17 (s, 6H, $-CH_3$), 4.26 (q, J=7.2 Hz, 4H, $-CO_2C\underline{H}_2CH_3$), 6.78–6.90 (m, 5H, Ar-H), 7.17–7.37 (m, 5H, Ar-H); ^{13}C-NMR (100 MHz, $CDCl_3$) δ: 14.4, 16.4, 60.4, 112.1, 113.3, 128.5, 128.9, 129.0, 129.3, 130.4, 138.4, 148.9, 150.5, 166.8; HR-MS (ESI) m/z: $[M+H]^+$ for $C_{24}H_{27}N_2O_4$: 407.1971 (Calcd), 407.1968 (Found).

3,5-Dimethyl-1-phenyl-4-(4-chlorophenyl)-1,4-dihydropyrazine-2,6-diethylmethanoate (**4-2**): Yellowish green solid (55%); mp 200.1–201.3°C; ^{1}H-NMR (400 MHz, $CDCl_3$) δ: 1.26 (*t*, 6H, J=7.2 Hz, $-CO_2CH_2C\underline{H}_3$), 2.18 (*s*, 6H, $-CH_3$), 4.26 (*q*, J=7.2 Hz, 4H, $-CO_2C\underline{H}_2CH_3$), 6.74–7.35 (*m*, 9H, Ar-H); ^{13}C-NMR (100 MHz, $CDCl_3$) δ: 14.4, 16.4, 60.4, 112.4, 113.2, 119.5, 128.5, 129.6, 131.7, 135.1, 136.9, 150.2, 150.9, 166.4; HR-MS (ESI) (m/z): $[M+H]^+$ for $C_{24}H_{26}ClN_2O_4$: 441.1581 (Calcd), 441.1587 (Found).

3,5-Dimethyl-1-phenyl-4-(4-methylphenyl)-1,4-dihydropyrazine-2,6-diethylmethanoate (**4-4**): Light yellow solid (55%); mp 201.5–202.7°C; ^{1}H-NMR (400 MHz, $CDCl_3$) δ: 1.28 (t, J=7.2 Hz, 6H, $-CO_2CH_2C\underline{H}_3$), 2.20 (s, 6H, $-CH_3$), 2.37 (s, 3H, Ar-CH_3), 4.27 (q, J=7.2 Hz, 4H, $-CO_2C\underline{H}_2CH_3$), 6.77–7.28 (m, 9H, Ar-H); ^{13}C-NMR (100 MHz, $CDCl_3$) δ: 14.4, 16.4, 21.1, 60.2, 111.6, 113.2, 119.2, 128.4, 129.9, 130.0, 135.7, 139.0, 150.8, 151.1, 166.6; HR-MS (ESI) (m/z): $[M]^+$ for $C_{25}H_{28}N_2O_4$: 420.2049 (Calcd), 420.2054 (Found).

3,5-Dimethyl-1-(4-chlorophenyl)-4-phenyl-1,4-dihydropyrazine-2,6-diethylmethanoate (**4-10**): Light yellowish green solid (63%); mp 217.5–218.3°C; ^{1}H-NMR (400 MHz, $CDCl_3$) δ: 1.28 (t, J=7.2 Hz, 6H, $-CO_2CH_2C\underline{H}_3$), 2.20 (s, 6H, $-CH_3$), 4.27 (q, J=7.2 Hz, 4H, $-CO_2C\underline{H}_2CH_3$), 6.69–7.41 (m, 9H, Ar-H); ^{13}C-NMR (100 MHz, $CDCl_3$) δ: 14.4, 16.5, 60.1, 111.4, 114.3, 124.0, 128.3, 129.0, 129.4, 130.3, 149.2, 149.4, 150.5, 166.1; HR-MS (ESI) (m/z): $[M^+]$ for $C_{24}H_{25}ClN_2O_4$: 440.1503 (Calcd), 440.1517 (Found).

3,5-Dimethyl-1,4-dis(4-chlorophenyl)-1,4-dihydropyrazine-2,6-diethylmethanoate (**4-11**): Light yellowish green solid (62%); mp 214.3–216.4°C; ^{1}H-NMR (400 MHz, $CDCl_3$) δ: 1.28 (t, J=7.2 Hz, 6H, $-CO_2CH_2C\underline{H}_3$), 2.20 (s, 6H, $-CH_3$), 4.26 (q, J=7.2 Hz, 4H, $-CO_2C\underline{H}_2CH_3$), 6.67–7.39 (m, 8H, Ar-H); ^{13}C-NMR (100 MHz, $CDCl_3$) δ: 14.3, 16.4, 60.4, 112.1, 114.3, 124.2, 128.4, 129.7, 131.6, 135.2, 136.7, 149.4, 150.5, 166.0; HR-MS (ESI) (m/z): $[M^+]$ for $C_{24}H_{24}Cl_2N_2O_4$: 474.1113 (Calcd), 474.1138 (Found).

3,5-Dimethyl-1-(4-chlorophenyl)-4-(4-methylphenyl)-1,4-dihydropyrazine-2,6-diethylmethanoate (**4-12**): Yellowish green solid (60%); mp 222.2–223.4°C; ^{1}H-NMR (400 MHz, $CDCl_3$) δ: 1.27 (t, J=7.2 Hz, 6H, $-CO_2CH_2C\underline{H}_3$), 2.16 (s, 6H, $-CH_3$), 2.31 (s, 3H, Ar-CH_3), 4.26 (q, J=7.2 Hz, 4H, $-CO_2C\underline{H}_2CH_3$), 6.67–7.37 (m, 8H, Ar-H); ^{13}C-NMR (100 MHz, $CDCl_3$) δ: 14.4, 16.4, 55.5, 111.3, 114.3, 114.5, 124.0, 128.3, 129.3, 130.6, 134.2, 149.7, 153.4, 159.7, 167.2; HR-MS (ESI) (m/z): $[M^+]$ for $C_{25}H_{27}ClN_2O_4$: 454.1659 (Calcd), 454.1668 (Found).

3,5-Dimethyl-1-(4-chlorophenyl)-4-(4-methoxyphenyl)-1,4-dihydropyrazine-2,6-diethylmethanoate (**4-14**): Yellowish green solid (59%); mp 128.6–129.3°C; ^{1}H-NMR (400 MHz, $CDCl_3$) δ: 1.28 (t, J=7.2 Hz, 6H, $-CO_2CH_2C\underline{H}_3$), 2.20 (s, 6H, $-CH_3$), 3.83 (s, 3H, Ar-OCH_3), 4.26 (q, J=7.2 Hz, 4H, $-CO_2C\underline{H}_2CH_3$), 6.68–7.28 (m, 8H, Ar-H); ^{13}C-NMR (100 MHz, $CDCl_3$) δ: 14.4, 16.4, 55.5, 60.3, 111.3, 114.3, 114.5, 124.0, 128.3, 129.3, 130.6, 131.2, 149.7, 151.4, 159.7, 166.2; HR-MS (ESI) (m/z): $[M]^+$ for $C_{25}H_{27}ClN_2O_5$: 470.1608 (Calcd), 470.1613 (Found).

3,5-Dimethyl-1-(4-methylphenyl)-4-phenyl-1,4-dihydropyrazine-2,6-diethylmeth-anoate (**4-19**): Yellow solid (33%); mp 220.3–221.5°C; ^{1}H-NMR (400 MHz, $CDCl_3$) δ: 1.26 (t, J=7.2 Hz, 6H, $-CO_2CH_2C\underline{H}_3$), 2.17 (s, 6H, $-CH_3$), 2.27 (s, 3H, Ar-CH_3), 4.25 (q, J=7.2 Hz, 4H, $-CO_2C\underline{H}_2CH_3$), 6.67–7.37 (m, 9H, Ar-H); ^{13}C-NMR (100 MHz, $CDCl_3$) δ: 14.4, 16.5, 20.5, 60.3, 112.1, 113.3, 128.5, 128.9, 129.0, 129.3, 130.4, 138.4, 148.9, 150.5, 166.8; HR-MS (ESI) (m/z): $[M]^+$ for $C_{25}H_{28}N_2O_4$: 420.2049 (Calcd), 420.2058 (Found).

3,5-Dimethyl-1-(4-methylphenyl)-4-(4-chlorophenyl)-1,4-dihydropyrazine-2,6-diethylmethanoate (**4-20**): Yellowish green solid (31%); mp 153.2.1–154.6°C; ^{1}H-NMR (400 MHz, $CDCl_3$) δ: 1.28(t, J=7.2 Hz, 6H, $-CO_2CH_2C\underline{H}_3$), 2.18 (s, 6H, $-CH_3$), 2.29 (s, 3H, Ar-CH_3), 4.26 (q, J=7.2 Hz, 4H, $-CO_2C\underline{H}_2CH_3$), 6.67–7.36 (m, 8H, Ar-H); ^{13}C-NMR (100 MHz, $CDCl_3$) δ: 14.3, 16.4, 20.5, 60.3, 112.8, 113.3, 128.6, 129.1, 129.5, 129.6, 131.7, 135.0, 137.0, 148.8, 150.0, 166.6; HR-MS (ESI) (m/z): $[M]^+$ for $C_{25}H_{27}ClN_2O_4$: 454.1659 (Calcd), 454.1672 (Found).

3,5-Dimethyl-1-(4-methylphenyl)-4-(4-methoxyphenyl)-1,4-dihydropyrazine-2,6-diethylmethanoate (**4-24**): Light yellow solid (29%); mp 171.1–172.4°C; ^{1}H-NMR (400 MHz, $CDCl_3$) δ: 1.26 (t, J=7.2 Hz, 6H, $-CO_2CH_2C\underline{H}_3$), 2.17 (s, 6H, $-CH_3$), 2.27 (s, 3H, Ar-CH_3), 3.80 (s, 3H, Ar-OCH_3), 4.24 (q, J=7.2 Hz, 4H, $-CO_2C\underline{H}_2CH_3$), 6.66–7.26 (m, 8H, Ar-H); ^{13}C-NMR (100 MHz, $CDCl_3$) δ: 14.4, 16.4, 20.5, 55.5, 60.2, 112.0, 113.3, 114.3, 128.4, 129.0, 130.9, 131.3, 149.0, 150.9, 159.6, 166.8; HR-MS. (ESI) (m/z): $[M]^+$ for $C_{26}H_{30}N_2O_5$: 450.2155 (Calcd), 450.2173 (Found).

3,5-Dimethyl-1,4-(4-ethoxycarbonylphenyl)-1,4-dihydropyrazine-2,6-diethylmethanoate (**4-60**): Light yellow solid (68%); mp 180.1–182.3°C; ^{1}H-NMR (400 MHz, $CDCl_3$) δ: 1.25 (t, J=7.2 Hz, 6H, Ar-$CO_2CH_2C\underline{H}_3$), 1.38 (t, 6H, $-CO_2CH_2C\underline{H}_3$), 2.21 (s, 6H, CH_3), 4.25 (q, J=7.2 Hz, 4H, $-CO_2C\underline{H}_2CH_3$), 4.36 (q, J=7.2 Hz, 4H, Ar-$CO_2C\underline{H}_2CH_3$), 6.70–8.07 (m, 8H, Ar-H); ^{13}C-NMR (100 MHz, $CDCl_3$) δ: 14.8, 16.5, 16.7, 59.8, 60.5, 61.5, 110.5, 116.1, 116.5, 121.3, 122.4, 124.7, 125.6, 131.3, 134.9, 149.8, 153.3, 159.7, 161.8; HR-MS-ESI (m/z): $[M]^+$ for $C_{30}H_{34}N_2O_8$: 550.2315 (Calcd), 550.2328 (Found).

3,5-Dimethyl-1,4-dis(3-nitrophenyl)-1,4-dihydropyrazine-2,6-diethylmethanoate (**4-61**): Light yellow solid (62%); mp 66.5–67.3°C; ^{1}H-NMR (400 MHz, $CDCl_3$) δ: 1.25–1.28 (t, J=7.2 Hz, 6H, $-CO_2CH_2C\underline{H}_3$), 2.24 (s, 6H, $-CH_3$), 4.29 (q, J=7.2 Hz, 4H, $-CO_2C\underline{H}_2CH_3$), 7.01–7.73 (m, 8H, Ar-H); ^{13}C-NMR (100 MHz, $CDCl_3$) δ: 14.8, 16.5, 60.4, 103.6, 104.2, 106.5, 107.8, 112.1, 124.6, 128.3, 129.5, 145.6, 146.9,

149.4, 150.8, 151.3, 152.5, 166.3; HR-MS-ESI (*m/z*): $[M]^+$ for $C_{24}H_{24}N_4O_8$: 496.1594 (Calcd), 496.1586 (Found).

Biological Assay The inhibition of the enzymatic activity of human 11β-HSD1 was determined through the scintillation proximity assay (SPA) using microsomes containing 11β-HSD1.[11,18] Briefly, the full-length cDNAs of human 11β-HSD1 were isolated from cDNA libraries provided by the NIH Mammalian Gene Collection and cloned into the pcDNA3 expression vector (Invitrogen, Carlsbad, CA, U.S.A.) by polymerase chain reaction (PCR). HEK293 cells were transfected with the pcDNA3-derived expression plasmids and selected by cultivation in the presence of 700 μg/mL G418. The microsomal fractions overexpressing 11β-HSD1 were prepared from HEK293 cells that were stably transfected with 11β-HSD1 and used as the enzyme source for SPA. The assay was performed in a 96-well microtiter plate. Different concentrations of the compounds were added, followed by the addition of 80 μL of 50 mmol/L *N*-(2-hydroxyethyl)piperazine-*N*′-2-ethanesulfonic acid (HEPES) buffer, pH 7.4, containing 25 nmol/L [1,2-(*n*)3*H*]cortisone (Amersham, Buckinghamshire, U.K.) and 1.25 mmol/L NADPH. The reactions were initiated by the addition of the 11β-HSD1 enzyme preparation as microsomal fractions from HEK293 cells to a final concentration of 80 μg/mL 11β-HSD1. After incubation for 60 min at 37°C, the reaction was stopped by the addition of 35 μL of 10 mg/mL protein A-coated SPA beads (GE, Piscataway, NJ, U.S.A.) suspended in Superblock® Blocking Buffer (Pierce, Rockford, IL, U.S.A.) with 3 μg/mL of murine monoclonal cortisol antibody (East Coast Biologics, North Berwick, Maine, U.S.A.) and 314 μmol/L glycyrrhetinic acid (Sigma-Aldrich, St. Louis, MO, U.S.A.). The plates were incubated under plastic film on an orbital shaker for 120 min at room temperature. The [^{3}H]-cortisol generated in the enzymatic reaction was captured by the beads and measured in a liquid scintillation counter equipped to read microplates. The percentage inhibition was calculated relative to an uninhibited control. The data were obtained from at least three independent experiments.

Acknowledgments This work was financially supported by the Key Projects of the National Science and Technology Pillar Program (No. 2012ZX10001007-008-002) and the Doctoral Fund of Innovation of Beijing University of Technology.

REFERENCES

1) Tomlinson JW, Walker EA, Bujalska IJ, Draper N, Lavery GG, Cooper MS, Hewison M, Stewart PM. 11β-Hydroxysteroid dehydrogenase type 1: a tissue-specific regulator of glucocorticoid response. *Endocr. Rev.*, **25**, 831–866 (2004).
2) Newell-Price J, Bertagna X, Grossman AB, Nieman LK. Cushing's syndrome. *Lancet*, **367**, 1605–1617 (2006).
3) Wang M. Tissue-specific glucocorticoid excess in the metabolic syndrome: 11β-HSD1 as a therapeutic target. *Drug Dev. Res.*, **67**, 567–569 (2006).
4) Masuzaki H, Paterson J, Shinyama H, Morton NM, Mullins JJ, Seckl JR, Flier JS. A transgenic model of visceral obesity and the metabolic syndrome. *Science*, **294**, 2166–2170 (2001).
5) Jump DB, Botolin D, Wang Y, Xu J, Christian B, Demeure O. Fatty acid regulation of hepatic gene transcription. *J. Nutr.*, **135**, 2503–2506 (2005).
6) Wamil M, Seckl JR. Inhibition of 11β-hydroxysteroid dehydrogenase type 1 as a promising therapeutic target. *Drug Discov. Today*, **12**, 504–520 (2007).
7) Sun D, Wang Z, Cardozo M, Choi R, Degraffenreid M, Di Y, He X, Jaen JC, Labelle M, Liu J, Ma J, Miao S, Sudom A, Tang L, Tu H, Ursu S, Walker N, Yan X, Ye Q, Powers JP. Synthesis and optimization of arylsulfonylpiperazines as a novel class of inhibitors of 11β-hydroxysteroid dehydrogenase type 1 (11β-HSD1). *Bioorg. Med. Chem. Lett.*, **19**, 1522–1527 (2009).
8) Wan ZK, Chenail E, Xiang J, Li HQ, Ipek M, Bard J, Svenson K, Mansour TS, Xu X, Tian X, Suri V, Hahm S, Xing Y, Johnson CE, Li X, Qadri A, Panza D, Perreault M, Tobin JF, Saiah E. Efficacious 11β-hydroxysteroid dehydrogenase type I inhibitors in the diet-induced obesity mouse model. *J. Med. Chem.*, **52**, 5449–5461 (2009).
9) Wan ZK, Chenail E, Li HQ, Kendall C, Wang Y, Gingras S, Xiang J, Massefski WW, Mansour TS, Saiah E. Synthesis of potent and orally efficacious 11β-hydroxysteroid dehydrogenase type 1 inhibitor HSD-016. *J. Org. Chem.*, **76**, 7048–7055 (2011).
10) Yan X, Wang Z, Sudom A, Cardozo M, DeGraffenreid M, Di Y, Fan P, He X, Jaen JC, Labelle M, Liu J, Ma J, McMinn D, Miao S, Sun D, Tang L, Tu H, Ursu S, Walker N, Ye Q, Powers JP. The synthesis and SAR of novel diarylsulfone 11β-HSD1 inhibitors. *Bioorg. Med. Chem. Lett.*, **20**, 7071–7075 (2010).
11) Mundt S, Solly K, Thieringer R, Hermanowski-Vosatka A. Development and application of a scintillation proximity assay (SPA) for identification of selective inhibitors of 11β-hydroxysteroid dehydrogenase type 1. *Assay Drug Dev. Technol.*, **3**, 367–375 (2005).
12) Yang H, Shen Y, Chen J, Jiang Q, Leng Y, Shen J. Structure-based virtual screening for identification of novel 11β-HSD1 inhibitors. *Eur. J. Med. Chem.*, **44**, 1167–1171 (2009).
13) Wan Z-K, Chenail E, Xiang J, Li H-Q, Ipek M, Bard J, Svenson K, Mansour TS, Xu X, Tian X, Suri V, Hahm S, Xing Y, Johnson CE, Li X, Qadri A, Panza D, Perreault M, Tobin JF, Saiah E. Efficacious 11β-hydroxysteroid dehydrogenase type I inhibitors in the diet-induced obesity mouse model. *J. Med. Chem.*, **52**, 5449–5461 (2009).
14) Chorvat RJ, Rorig KJ. Synthesis of 4-aryl-3,5-bis(alkoxycarbonyl)-1,4-dihydropyrazines. *J. Org. Chem.*, **53**, 5779–5781 (1988).
15) He J-Y, Song X-Q, Yan H, Zhong R-G. New highlights in the synthesis of 4-aryl-1,4-dihydropyrazines. *J. Heterocycl. Chem.*, **49**, 1357–1361 (2012).
16) Sit SYHY, Antal-Zimanyi I, Ward S, Poindexter GS. Novel dihydropyrazine analogues as NPY antagonists. *Bioorg. Med. Chem. Lett.*, **12**, 337–340 (2002).
17) Mel'nik MV, Kornilov MY, Turov AV, Gutsulyak BM. Study of the cyclization of primary aromatic amines with formaldehyde and dimedone in the presence of perchloric acid. *Zhurnal Organicheskoi Khimii*, **18**, 1460–1466 (1982).
18) Xia G, Liu L, Xue M, Liu H, Yu J, Li P, Chen Q, Xiong B, Liu X, Shen J. Discovery of novel sulfonamides as potent and selective inhibitors against human and mouse 11beta-hydroxysteroid dehydrogenase type 1. *Mol. Cell. Endocrinol.*, **358**, 46–52 (2012).